J. Membrane Biol. 157, 255–269 (1997)

The Journal of
Membrane
Biology

Identification of Anion-selective Channels in the Basolateral Membrane of Mitochondria-rich Epithelial Cells

N.J. Willumsen, E.H. Larsen

Zoophysiological Laboratory, The August Krogh Institute, The University of Copenhagen, Universitetsparken 13, DK-2100 Copenhagen Ø, Denmark

Received: 10 October 1996/Revised: 8 January 1997

Abstract. Epithelial cells of toad (*Bufo bufo*) skin were isolated by treatments of the epidermis with collagenase and trypsin. Cl^- channels in the basolateral membrane from soma or neck of mitochondria-rich cells were studied in cell-attached and excised inside-out configurations. Of a total of 87 sealed patches only 28 (32%) were electrically active, and in these we identified four different types of Cl^- channels. The two major populations constituted Ohmic Cl^- channels with limiting conductance ($\gamma_{125/125}$) of 10 pS and 30 pS, respectively. A much rarer 150 pS Ohmic Cl^- channel was also characterized. From *i/V* relationships of individual channels the following Goldman-Hodgkin-Katz permeabilities were calculated, 2.2 (±0.1) × 10^{-14}, 5.7 (±0.7) × 10^{-14}, and 32 (±2) × 10^{-14} cm^3/sec, for the 10, 30 and 150 pS Cl^- channels, respectively. The 30 pS channel was activated by hyperpolarization. The gating kinetics of the 150 pS channel was complex with burstlike closures within openings of long duration. The fourth type of Cl^- channel was studied in patches generating 'noisy currents' with no discrete single-channel events, but with vanishing fluctuations at pipette potentials near E_{Cl}. Noise analysis revealed a power spectrum with cutoff frequencies of 1.2 and 13 Hz, indicating that resolution of kinetic steps was limited by small channel currents rather than fast channel gating. From the background noise level we estimated the channel conductance to be less than 1.7 pS. Despite the fact that the majority of patches did not contain electrically active Cl^- channels, patches being active, generally, contained more than a single active channel. Thus, for the above three types of resolvable channels, the mean number of active channels per patch amounted to 2.1, 1.4, and 2.0, respectively. This observation, like the finding of few patches with several unresolvable channels, indicates that electrically active Cl^- channels are organized in clusters.

Key words: Patch clamp — Noise analysis — Clusters of Cl^- channels — Unresolvable Cl^- channels

Introduction

The major Cl^- conductive pathway of the amphibian skin is controlled by the transepithelial potential (Larsen & Kristensen, 1978), the external Cl^- concentration (Harck & Larsen, 1986), and the intracellular cAMP concentration (Willumsen, Vestergaard & Larsen, 1992). It appears to be located to mitochondria-rich (MR[1]) cells (Voûte & Meier, 1978; Foskett & Ussing, 1986; Katz & Scheffey, 1986; Willumsen & Larsen, 1986; Larsen, Ussing & Spring, 1987; Larsen & Harvey, 1994; Rick 1994). In toad skin, this cell type contributes only by 2–5% to the total epithelial surface area suggesting a very large anion conductance of its plasma membranes. Thus, measured Cl^- currents carried by individual cells (Foskett & Ussing, 1986) or an ensemble of cells of known number (Willumsen & Larsen, 1986), lead to the conclusion that the apical membrane of MR cells ranks among the most conductive membranes known comparable to, e.g., chloride cells of teleost gill (Foskett et al., 1983), human sweat duct (Bijman & Frömter, 1986), and the nodes of frog myelinated axons (Hille, 1984). Also at very low, freshwater-like external Cl^- concentrations, when uptake of Cl^- is an active process (Krogh, 1937),

Correspondence to: N.J. Willumsen

[1] *Abbreviations:* MR cell, mitochondria-rich cell; GHK, Goldman-Hodgkin-Katz; CFTR, cystic fibrosis transmembrane conductance regulator; MDCK cells, Madin-Darby canine kidney cells; PKA, cAMP-dependent protein kinase A.

the MR cells constitute the transepithelial pathway for the Cl^- fluxes (Larsen, Willumsen & Christofferson, 1992, Jensen et al., 1997). The uptake of Cl^-, whether passive or active, necessarily encounter two transport barriers, namely the apical and the basolateral membranes of the mitochondria-rich cells. Although the area of the basolateral membrane is larger than that of the apical membrane, a high Cl^- permeability of the basolateral MR cell membrane is still to be expected. Due to the relative inaccessibility of the MR cells in the intact amphibian skin, however, conventional microelectrode technique cannot be applied for investigating conductive properties of the individual barriers, and little has until recently been revealed about individual membrane proteins responsible for translocation of Cl^- ions across the cell membranes.

A previous study of whole cell currents confirmed that toad skin MR cells expresses a significant Cl^- conductance (Larsen & Harvey, 1994). A more recent patch-clamp study identified Cl^- channels in the apical membranes of isolated MR cells (Sørensen & Larsen, 1996). Here, we present a study of the anion channels supposed to be involved in the subsequent translocation of Cl^- across the basolateral membrane. Parts of the study have been presented as brief reports (Willumsen & Larsen, 1995; Larsen et al., 1995; Willumsen & Larsen, 1996).

Materials and Methods

Preparation of Isolated Mitochondria-Rich Cells

Toads (*Bufo bufo*) were maintained at room temperature with access to a pool of tap water and meal worms. To increase the density of MR cells, five to seven days prior to the experiment the toads were transferred to either distilled water or 100 mM $NaNO_3$ (Willumsen & Larsen, 1986; Katz & Gabbay, 1988). This treatment resulted in a significantly higher yield of MR cells in the final preparation as compared to preparations from untreated animals. After decapitation and pithing, the skin was dissected free and the MR cell preparation was obtained according to Larsen and Harvey (1994). In brief, the epithelium was gently isolated from the underlying dermis after 1½–2 hr serosal exposure to 2 mg/ml collagenase (cat. no. 103568, Boehringer-Mannheim GmbH, Mannheim, Germany) in toad Ringer's solution. The isolated epithelium was subsequently transferred to 2 mg/ml Collagenase A1 (C9891, Sigma, St. Louis, MO) in toad Ringer. After 1 hr the isolated epithelium was washed twice in Ca^{2+}-free Ringer and transferred to 0.1 mg/ml trypsin (17072-018, Trypsin 1;250 USP grade, Life Technologies Ltd. Paisley, UK) for 3 min. The last mentioned procedure was repeated 5–10 times yielding sequential fractions of isolated epithelial cells. Each fraction was washed for 2 min in Ca^{2+}-free Ringer, centrifuged at 800–900 rpm for 5 min, and subsequently resuspended in 1-ml 'modified Ringer'. At this point the cells were ready for use. Generally, fractions 1–2 contained mostly small spherical cells, typical of the stratum germinativum. The later fractions contained a mixture of cell types including a large number of flat polygonal cells from the stratum corneum. Typically, the highest yield of MR cells was found in fractions 5–8. MR cells generally constituted 1:1000 or less of the total cell number which ranged from nil to ~10^8 cells/ml with 10^7 cells/ml as the representative order of magnitude.

Patch-Clamp Technique

Patch pipettes were pulled from borosilicate glass tubes with an internal filament (CG150F-15, Clark Electromedical Instruments, Reading, UK) on a horizontal DMZ-puller (Zeitz Instruments, Augsburg, Germany). After fire polishing, the pipette was backfilled with the desired pipette solution and mounted on the headstage of the patch-clamp amplifier. When filled with 'modified Ringer' the resistance of the patch pipette was 5–10 MΩ. The tip diameter was approximately 1 μm, *see* Fig. 1*A*. A sample of cells was suspended in 1–2 ml 'modified Ringer' in a 4-cm Petri dish (Nunc, Roskilde, Denmark) and positioned on the stage of an inverted microscope (Nikon Diaphot 300, Tokyo, Japan) placed on an anti-vibration table (Newport, Irvine, CA) inside a Faraday cage. After settling on the bottom of the Petri dish, the cells were inspected under low magnification (×100). When an MR cell had been identified by its distinct flasklike appearance (Fig. 1*B*) the magnification was increased to 400× using a 40× Hofman Modulation objective (HMC 40 LWD, Modulation Optics, Greenvale, NY) with 2.4-mm working distance. Under microscopic inspection the tip of the patch pipette was positioned within 70 μm from the MR cell by a manual micromanipulator. Subsequently, the tip of the patch pipette was brought into contact with the basolateral MR cell membrane (Fig. 1*B*) by a remote controlled 3-axis piezo-electric micromanipulator (Burleigh PCS-250, Fishers, NY) with a working distance of 70 μm. After contact, a slight negative hydrostatic pressure (−10 to −40 mP) was applied to the pipette to facilitate gigaseal formation. Pipette hydrostatic pressure was monitored by a digital manometer (500PL Eirelec, Dundalk, Ireland). Gigaseals, typically with a resistance of 10–60 GΩ, were obtained in approximately 5% of all attempts. Furthermore, patches were often short-lived lasting for less than 10 min. All experiments were carried out at room temperature (20–23°C), and channels were studied in cell-attached and excised inside-out configurations.

To record single-channel currents we used an RK-400 (Biologic, Claix, France) patch-clamp amplifier furnished with a 10 GΩ feedback resistor in the headstage (gain 100 or 200 mV/pA). Patch currents were monitored on an oscilloscope (VC-6023, Hitachi Denshi, Tokyo, Japan) and recorded on digital tape with 40 kHz bandwidth (Biologic DTR 1204). For analysis, currents were played back, low-pass filtered at 100–500 Hz by an 8-pole Bessel filter (Frequency Devices 901, Haverhill, MA), and digitized at a rate of 1 or 2 kHz by a CED 1401*plus* interface (Cambridge Electronic Design, Cambridge, UK). For controlling clamping voltage and for digitizing and analyzing clamping currents, the CED patch- and voltage clamp software (Version 6.2, Cambridge Electronic Design) was used.

Solutions

Standard Ringer (used for cell isolation) contained (in mM): 116 Na^+, 3.7 K^+, 1 Ca^{2+}, 118.7 Cl^-, 4 SO_4^{2-}, 3 acetate, 11 glucose, 8 Tris (pH = 7.4). Ca^{2+}-free Ringer (used for cell isolation): 116 Na^+, 3.7 k^+, 1 Ca^{2+}, 116.7 Cl^-, 4 SO_4^{2-}, 3 acetate, 11 glucose, 10 EGTA, 8 Tris (pH = 7.4), 'Modified Ringer' (used for cell isolation, as bath, and as pipette solution): 116 Na^+, 3.7 K^+, 4 Ca^{2+}, 124.7 Cl^-, 4 SO_4^{2-}, 3 acetate, 11 glucose, 8 Tris (pH = 7.2). 'Low Cl^- high K^+ Ringer' (used as pipette solution): 119.7 K^+, 4 Ca^{2+}, 41.6 Cl^-, 83.1 gluconate, 4 SO_4^{2-}, 3 acetate, 11 glucose, 8 Tris (pH = 7.4). The composition of the latter solution was chosen to facilitate identification of the ion species being

translocated through a channel. Thus with this solution in the pipette and 'modified Ringer' in the bath, equilibrium potentials (bath relative to pipette) should amount to, $+\infty$, -87.6 and 27.6 mV for Na^+, K^+ and Cl^-, respectively, for excised inside-out patches.

In some experiments, 1 mM Ba^{2+} was added to the bath solution to abolish the activity of basolateral K^+ channels.

Single-Channel Currents and Conductances

The current through single Cl^- channels (i_{Cl}) was found to obey the Goldman-Hodgkin-Katz (GHK) current equation (Goldman, 1943; Hodgkin & Katz, 1949):

$$i_{cl} = F \cdot \zeta \cdot P_{cl} \cdot V_m \cdot \frac{[Cl^-]_o - [Cl^-]_c \cdot \exp(-\zeta \cdot V_m)}{1 - \exp(-\zeta \cdot V_m)} \quad (1)$$

where P_{Cl} is the permeability coefficient, $[Cl^-]_o$ the Cl^- concentration in the pipette, $[Cl^-]_c$ the Cl^- concentration in the cell (cell-attached configuration) or in the bath (excised inside-out configuration), V_m the membrane potential (referenced to the pipette potential, $\Psi_c - \Psi_o$), and $\zeta = F/RT = 39.36$ C/J (at 23°C) where F, R, and T have their usual meanings. Recorded patch currents were fitted by the GHK equation using the following expression for V_m (Neher, 1992):

$$V_m = -V_p + V_c + V_{lj} \quad (2)$$

where V_p is the pipette potential measured relative to the bath ($\Psi_p - \Psi_b$), i.e., the clamp potential measured relative to the zero-current potential obtained by nulling external potential-offsets prior to the experiment, V_c is the spontaneous membrane potential ($\Psi_c - \Psi_b$, zero for inside-out patches), and V_{lj} is the liquid junction potential caused by electrolyte concentration gradients between electrodes and external medium (cytoplasm or bath). V_{lj} is indicated as bath potential relative to pipette, and is zero for excised inside-out patches exposed to symmetrical solutions. The value of V_{lj} with 'modified Ringer' outside and 'low Cl^- high K^+ Ringer' in the pipette was calculated according to Barry and Lynch (1991), $V_{ij} = 7.5$ mV.

According to Eq. 1, i_{Cl} would exhibit outward rectification when $[Cl^-]_c < [Cl^-]_o$ which is the case in cell-attached patches with 'modified Ringer' in the patch pipette. In the case of excised inside-out patches studied with 'low Cl^- high K^+ Ringer' in the pipette, $[Cl^-]_c > [Cl^-]_o$, and inward rectification is, therefore, expected.

The single-channel (integral) conductance, γ, was calculated from the equation (Finkelstein & Mauro, 1963):

$$\gamma = F \cdot \zeta^2 \cdot P_{Cl} \cdot V_m \cdot \frac{[Cl^-]_o - [Cl^-]_c \cdot \exp(-\zeta \cdot V_m)}{(1 - \exp(-\zeta \cdot V_m))} \Bigg/ ln\left(\exp(-\zeta \cdot V_m)\frac{[Cl^-]_c}{[Cl^-]_o}\right) \quad (3)$$

To compare conductances determined with 125 and 42 mM Cl^- in the pipette, the conductance obtained with $[Cl^-]_c/[Cl^-]_o = 125/42$ mM was converted into the limiting conductance ($\gamma_{125/125}$) by the equation:

$$\gamma_{C/C} = F \cdot \zeta \cdot P_{Cl} \cdot [Cl^-] \quad (4)$$

where P_{Cl} was obtained from the GHK-fit, and $[Cl^-] = 125$ mM. At the equilibrium potential for Cl^- (E_{Cl}), the conductance (γ_{eq}) was calculated from the equation:

$$\gamma_{eq} = -F \cdot \zeta^2 \cdot P_{Cl} \cdot E_{Cl} \cdot \frac{[Cl^-]_o \cdot [Cl^-]_c}{[Cl^-]_o - [Cl^-]_c} \quad (5)$$

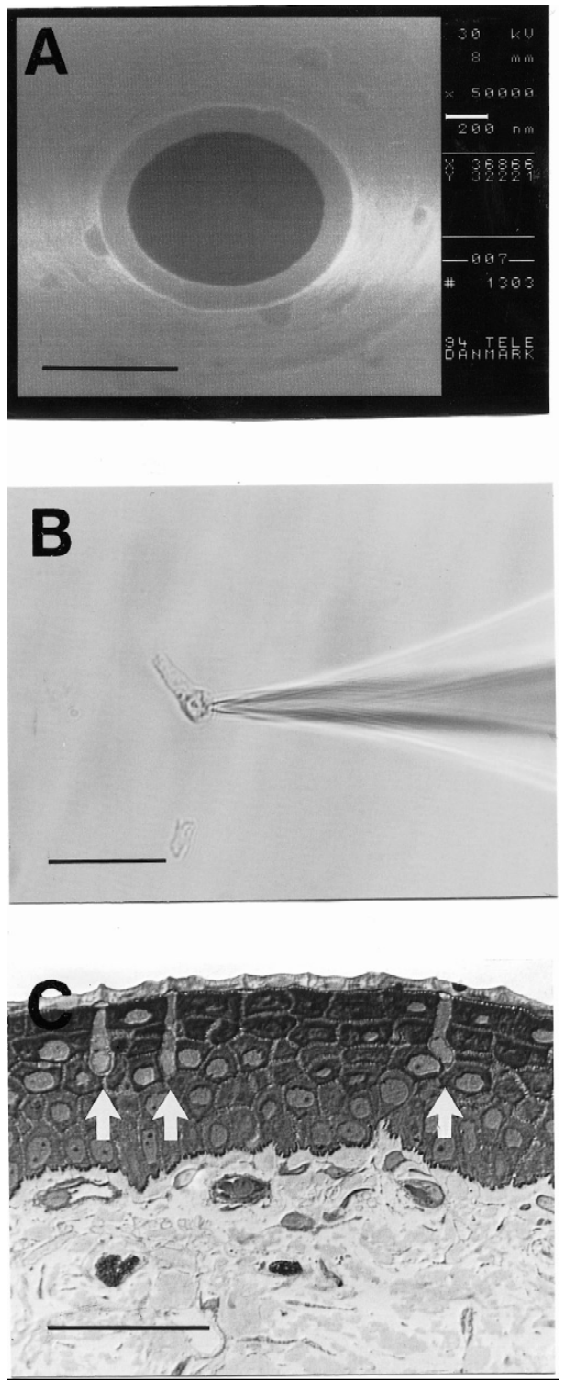

Fig. 1. (*A*) Scanning electron micrograph of patch pipette tip. Bar indicates 500 nm. (*B*). Patch pipette in contact with the basolateral membrane of an isolated mitochondria-rich cell. Bar indicates 25 μm. (*C*) Transection of toad skin epidermis containing three MR cells (arrows) interspersed between dark-colored principal cells. Bar indicates 50 μm. (Courtesy Dr. P.E. Budtz).

The single-channel slope conductance (γ_{slope}) in the point (V_m, i_{Cl}) was calculated from the equation (Willumsen & Boucher, 1989):

$$\gamma_{slope} = \frac{i_{Cl}}{V_m} - \tfrac{1}{2} \cdot F \cdot \zeta^2 \cdot P_{Cl} \cdot V_m \cdot \frac{[Cl^-]_o - [Cl^-]_c}{\cosh(\zeta \cdot V_m) - 1} \quad (6)$$

The open-state probability (P_o) was determined from the fitted Gaussian distributions of the single-channel currents by the equation:

$$P_o = \frac{1}{N_{\text{obs}}} \cdot \sum_{j=1}^{N} j \cdot P_j = \frac{1}{N_{obs}} \cdot \sum_{j=1}^{N} j \cdot A_j \quad (7)$$

where N_{obs} is the maximal number of active channels observed in the patch at any time or potential, N is the number of channels observed in the recording considered (i.e., $1 \leqslant N \leqslant N_{\text{obs}}$), P_j is the probability of j channels being open at a time, and A_j is the relative area under the j'th Gaussian curve (supposing that the Gaussian curve corresponding to the all-channels-closed state is designated, '$j = 0$').

Analysis of Variance and Spectral Density of Stationary Current Fluctuations

Analysis of fluctuations of currents with no resolvable channel transitions were performed with the SPAN program (J. Dempster, Strathclyde Electrophysiology, Glasgow, UK). Currents which were stored on the digital tape recorder (single-channel recording mode, 10 GΩ feed-back resistor, 50 mV/pA; bandwidth 40 kHz) were low-pass filtered at, f_c = 500 Hz (−3 dB, eight-pole Bessel), further amplified (gain ×10), and digitized at 1-msec intervals. The spectrum of current fluctuations covering a frequency range of 0.244–500 Hz (Fig. 8*D*) was calculated by a 4096-points fast Fourier transformation multiplied by a 10% cosinus bell window time function. Each spectrum was obtained by averaging such 4–5 individually transformed records of a continuous stationary current segment (V_p held constant, total length of current segment, ~20 sec). Lorentzian functions, $S(f)$, were fitted to the calculated spectrum using the Levenberg-Marquardt nonlinear least-square routine:

$$S(f) = \frac{S_0}{1 + (f/f_c)^2} \quad (8)$$

where S_0 is the low-frequency asymptote with the corner frequency defined by, $S(fc) = ½S_0$.

The mean current (i) used for calculation of the variance of the fluctuations (σ^2) was obtained by simultaneous sampling and digitizing of the low-pass filtered signal (as above) through a DC-coupled channel (gain ×1). Thus, for each record,

$$\sigma^2 = \frac{1}{n-1} \sum_{j=1}^{n} (\bar{i} - i_j)^2 \quad (9)$$

where, i_j is the value of a discrete digitized current point, and n the number of sampled current points in the record. With a sampling interval of 1 msec and a time record length of 1024 msec, n = 1024. The estimate of σ^2 (Fig. 7*A–C*) was obtained as the mean ± standard error of the mean (SEM) of 17–18 records.

The contribution of individual Lorentzian components to the total variance of current fluctuations (Table 1) was obtained by integration of the Lorentzian function,

$$\sigma^2 = \int_0^\infty \frac{S_0}{1 + (f/f_c)^2}\, df = ½\pi \cdot f_c \cdot S_0 \quad (10)$$

The relaxation time constants of the current fluctuations were calculated according to:

$$\tau = \frac{1}{2 \cdot \pi \cdot f_c} \quad (11A)$$

from which the mean open dwell-time can be calculated by:

$$\tau_{\text{open}} = \frac{\tau}{1 - P_o} \quad (11B)$$

Results

The isolated MR cells were easily identified due to their characteristic flasklike appearance which was maintained after the isolation. Channel activity was demonstrated in 28 out of 87 basolateral membrane patches ('active patches') which were obtained either from the soma (N = 56) or from the neck region (N = 31) of isolated MR cells. However, due to rundown or short gigaseal lifetime, only data from 23 patches were considered suitable for detailed analysis. Twenty one active patches contained a grand total of 36 individual, resolvable Cl^- channels. Eleven patches contained a single channel, four patches contained two channels, five patches contained three channels, and a single patch contained four channels.

Clearly, the channels detected did not belong to a single common class, but exhibited distinct heterogeneity. Figure 2 presents data from an excised inside-out basolateral membrane patch exposed to bilateral 'modified Ringer' solutions. Single-channel currents are depicted against $-V_p$ which in this configuration equals the membrane potential. Obviously, the patch contained more than a single Cl^- channel type, and based on the slopes of the $i_{Cl}/-V_p$ relations three types of channels could be identified with single-channel conductances of 8.3, 22.2, and 34.3 pS, respectively. Note that the intermediate 22.2 pS channel was observed at negative $-V_p$ values, only. Original current traces recorded at pipette potentials of 60 and −80 mV are shown in the middle panels of Fig. 2, and the bottom panels illustrate distinct Gaussian distributions of the recorded patch currents.

Small Chloride Channels

In studies with 'modified Ringer' or 'low Cl^- high K^+ Ringer' in the patch pipette, a small, linear channel of approximately 10 pS ($\gamma_{125/125}$, Eq. 4) was most often encountered. The 10 pS Cl^- channel was detected in 10 patches containing a grand total of 20 channels. The number of channels per active patch varied from 1 to 3 with a mean of 2.0 ± 0.3. Eight channel-containing patches were obtained from the soma region, and one from the neck region. The 10 pS channel, which was active at positive as well as negative pipette potentials, was characterized by a linear $i_{Cl}/-V_p$ relation when exposed to symmetrical 'modified Ringer' solutions as illustrated in Fig. 2 in an experiment with an excised inside-out patch. In Fig. 3 are shown results from an experiment in which the pipette solution had been reduced

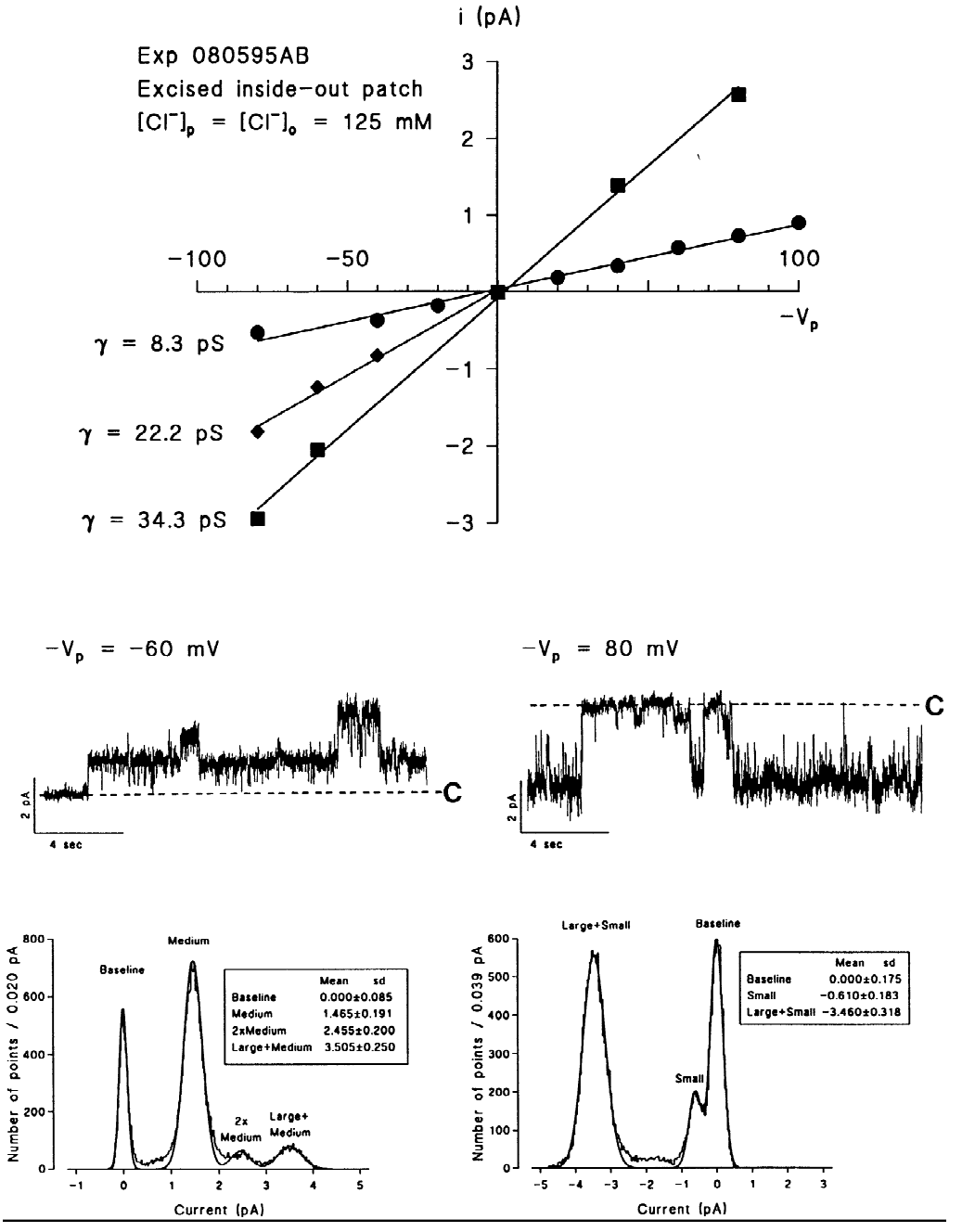

Fig. 2. Excised inside-out recordings from a basolateral membrane patch on a mitochondria-rich cell. 'Modified Ringer' ([Cl^-] = 125 mM) was used as pipette- and bath solutions. The figure illustrates the heterogeneity of the Cl^- channels observed. In the upper panel is presented 3 linear $i_{Cl}/-V_p$ relations with slopes of, γ = 8.3, 22.2, and 34.3 pS, respectively. Recorded currents are depicted as a function of the negative pipette potential ($-V_p$). Middle panel depicts original single-channel recordings (positive currents downward). The closed level is denoted 'C'. The lower panel shows the distributions of the currents depicted in the middle panel with lines indicating Gaussian fits with means and SDs listed.

to 42 mM Cl^-. In this case the single-channel current exhibited a marked outward rectification and the $i_{Cl}/-V_p$ relation could be fitted by the GHK equation (Eq. 1). In the interval, −100 mV < $-V_p$ < 100 mV, γ_{slope} varied from 8.8 to 3.4 pS, and at the reversal potential the conductance was, γ_{rev} = 6.3 pS. The reversal potential was within, 10 mV < $-V_p$ < 20 mV, i.e., closer to the equilibrium potential for Cl^-, E_{Cl} = +27.5 mV, than to that of K^+, E_K = −87.6 mV. The single-channel conductance ranged from 8.3 to 13.4 pS, and the mean conductance ($\gamma_{125/125}$) obtained for this Cl^- channel amounted to 10.5 ± 0.6 pS, with a mean P_{Cl} of 2.2 (±0.1) · 10^{-14}

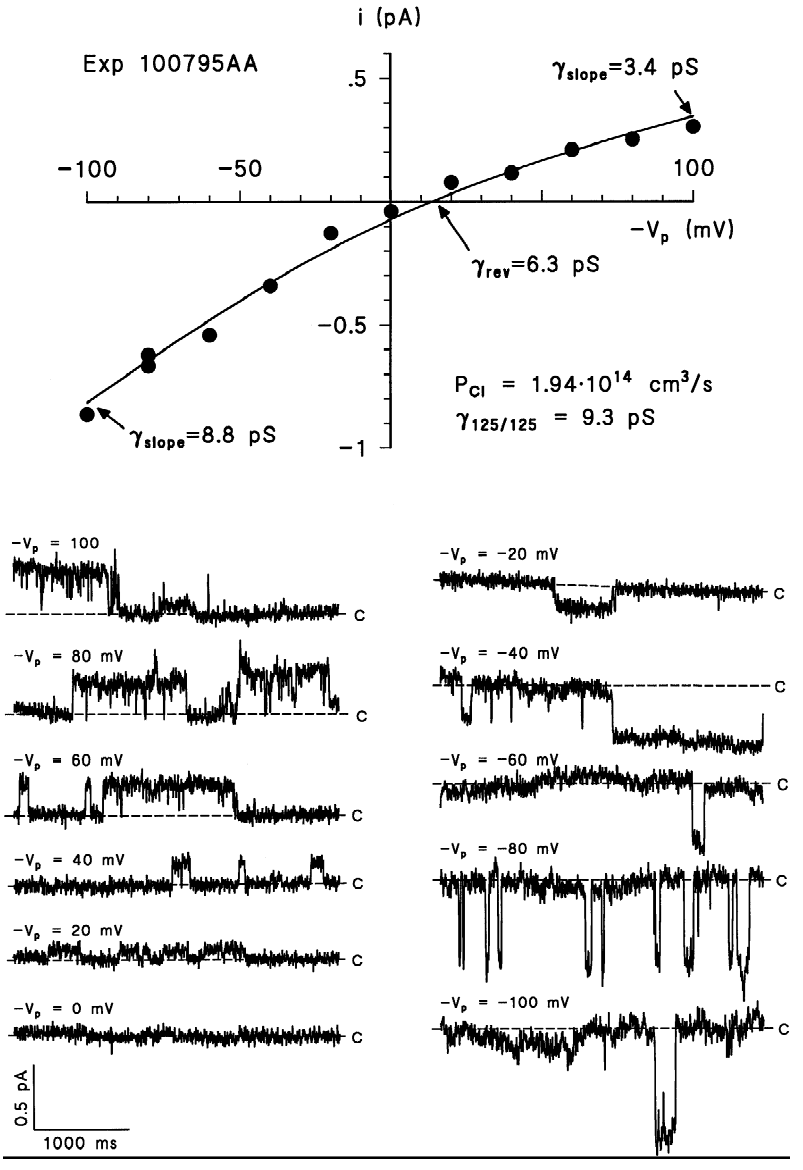

Fig. 3. Single-channel currents recorded from a excised inside-out patch from the basolateral membrane containing a single small Cl^- channel. Patch pipette solution contained 42 mM Cl^- and the bath solution contained 125 mM Cl^-. The full line is the best GHK fit (Eq. 1) which was obtained with $P_{Cl} = 1.94 \times 10^{-14}$ cm^3/sec, which translates into a $\gamma_{125/125}$ (Eq. 4) of 9.3 pS. Lower panel shows 11 original single-channel current records at potentials ($-V_p$) ranging from −100 to 100 mV.

cm^3/sec (mean ± SEM, $N = 10$). The lack of any effect of 1 mM Ba^{2+} added to the bath (*not shown*) served to support the conclusion that this channel was not a basolateral K^+ channel. The activity of the channel was not affected by negative hydrostatic pressure in the pipette (range tested: 0 to −40 mP, *not shown*). The 10 pS Cl^- channel was active at both negative and positive $-V_p$, and the open-state probability (P_o) typically amounted ~0.5 without any significant voltage-dependence.

Intermediate Chloride Channels

Also a larger, ~30 pS Cl^- channel was regularly observed. Fig. 4 depicts the $i_{Cl}/-V_p$ relation obtained in a cell-attached patch with 'low Cl^- high K^+ Ringer' as pipette solution, and examples of patch currents recorded at various pipette potentials are shown in the lower panels of Fig. 4. From the GHK-fit we obtained a single-channel permeability, $P_{Cl} = 8.7 \times 10^{-14}$ cm^3/sec, and the following estimates of cellular parameters: $[Cl^-]_c = 18.0$ mM, and $V_c = -30.5$ mV. Subsequently, the patch was excised and studied in the inside-out configuration. The result is shown in Fig. 5. Following excision, the curvature of the $i_{Cl}/-V_p$ relation reversed and the reversal potential shifted polarity, approaching the equilibrium potential for Cl^-. The optimal GHK-fit was obtained for $P_{Cl} = 5.9 \times 10^{-14}$ pS, corresponding to $\gamma_{125/125} = 28$ pS and $\gamma_{rev} = 15.2$ pS. In the interval, -100 mV $< -V_p < 80$ mV, γ_{slope} decreased from 26.5 to 11.1 pS.

The 30 pS channel was detected in 9 patches containing a total of 13 copies of the channel. The number of channels per patch varied from 1 to 4 with a mean of

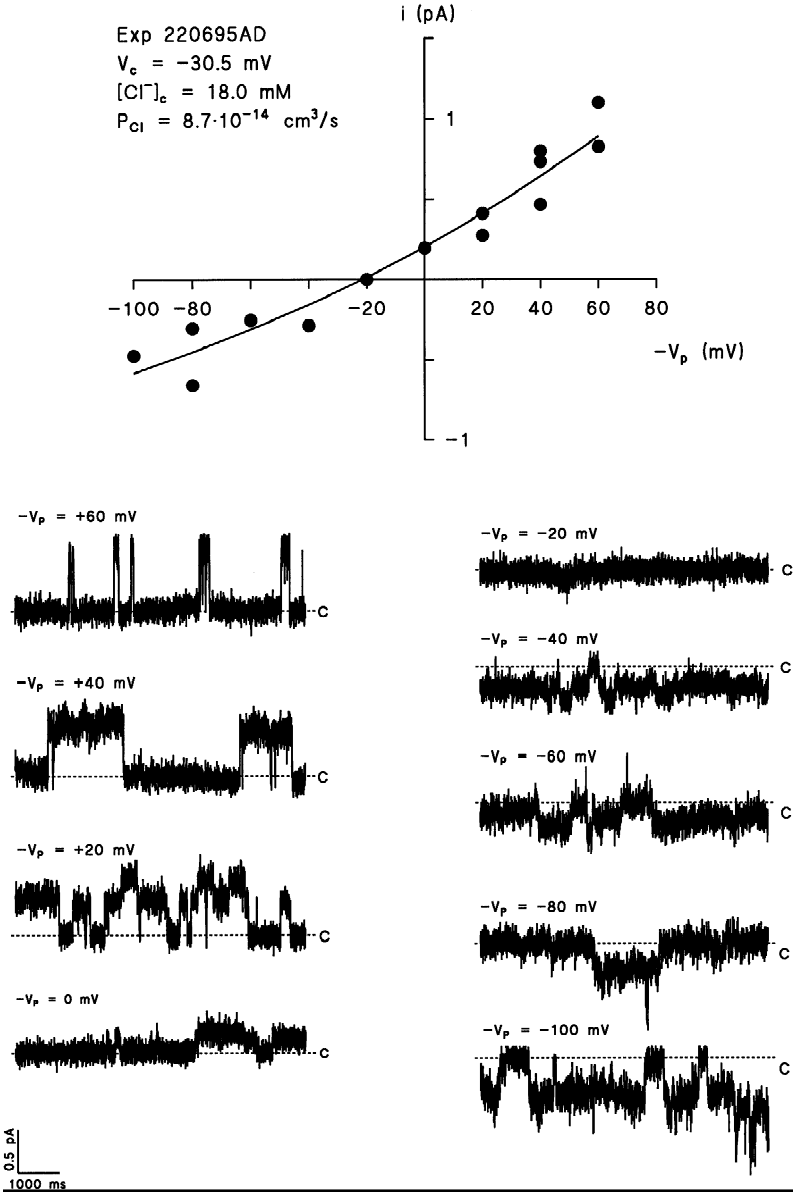

Fig. 4. Cell-attached recordings from a patch containing two intermediate Cl^- channels. Pipette solution contained 42 mM Cl. The best GHK fit was obtained with V_c = −30.5 mV, $[Cl^-]_c$ = 18 mM, and P_{Cl} = 8.7 × 10^{-14} cm^3/sec. Lower panel presents digitized single-channel current traces.

1.4 ± 0.3. Four channel-containing patches were obtained from MR cell soma region and two from the neck region. The conductance ($\gamma_{125/125}$) of the intermediate Cl^- channel ranged from 22.2 to 34.9 pS with a mean value of 30.6 ± 1.4 pS (N = 8). The mean P_{Cl} amounted to 5.7 (±0.7) · 10^{-14} cm^3/sec. Like the small channel, neither was the activity of the 30 pS channel affected by lowering of the hydrostatic pressure in the pipette (*not shown*).

Generally, the 30 pS Cl^- channels studied appeared most active at negative $-V_p$ values, i.e., at hyperpolarized membrane potentials (as also seen in Fig. 5). In some cases, P_o was so low at positive $-V_p$ values that no channel openings were recorded so that a single-channel current could not be determined, *see* e.g., Fig. 1. The voltage-dependence of the channel activity is illustrated in Fig. 6. Typically, P_o varied between 0.5–0.8 at large negative $-V_p$ values and 0–0.2 at positive $-V_p$ values.

Large Chloride Channels

In two cell-attached patches four very large channels were observed. The $i_{Cl}/-V_p$ relation for this type of channel, obtained in cell-attached patch configuration with 'modified Ringer' in the bath, is shown in Fig. 7, upper panel. Single-channel currents recorded at $-V_p$ values between −30 and 100 mV are presented in Fig. 7, lower panels. Note, that the patch contained two large Cl^- channels and one intermediate Cl^- channel. The data could not be fitted with the GHK equation expressed for

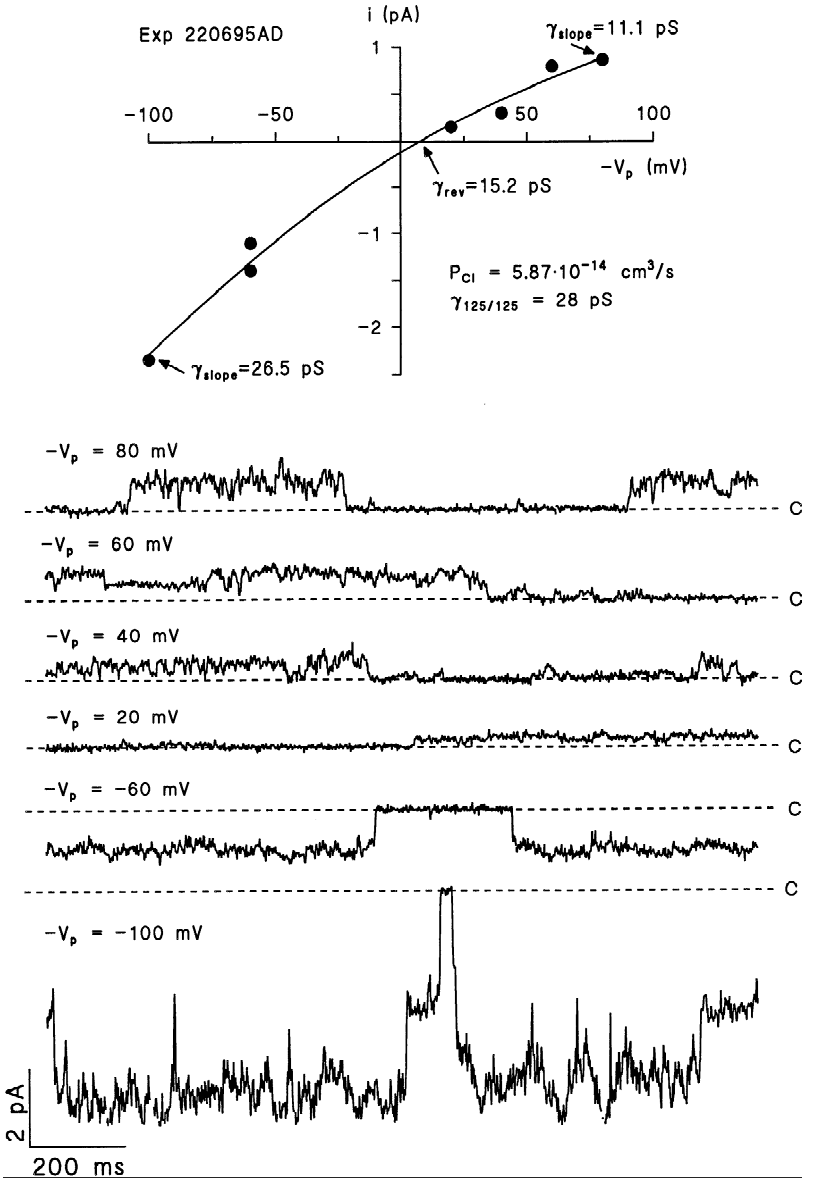

Fig. 5. Data from the same patch as the one presented in Fig. 4 after excision into a Ringer solution containing 42 mM Cl^-. The $i_{Cl}/-V_p$ relation for the intermediate Cl^- channel was fitted with the GHK equation and the best fit was obtained with $P_{Cl} = 5.9 \times 10^{-14}$ cm^2/sec. Lower panel shows the single-channel currents on an expanded time scale.

cations ($z = +1$ and the known concentrations extracellular Na^+ or K^+ concentrations), but was nicely fitted when using parameters for Cl^- ($z = -1$ and $[Cl]_o = 125$ mM). The best GHK-fit was obtained with $[Cl^-]_c = 31.7$ mM, $V_c = -37.8$ mV, and a permeability coefficient of, $P_{Cl} = 29.4 \times 10^{-14}$ cm^3/sec. Thus, the limiting conductance, $\gamma_{125/125} = 141$ pS. For four channels in two preparations the mean permeability coefficient amounted to, $P_{Cl} = 32\ (\pm 2) \times 10^{-14}$ cm^3/sec, corresponding to $\gamma_{125/125} = 154 \pm 9$ pS ($N = 4$). The fact that the reversal potential for i_{Cl} was indistinguishable from zero is in agreement with the notion (Larsen et al., 1987), that Cl^- is distributed at equilibrium across the basolateral membrane of the mitochondria-rich cell. Due to the scarcity of observations of the large Cl^- channel, we were not able to firmly establish whether or not its gating is voltage sensitive. If anything, the large Cl^- channel appeared most active at large positive $-V_p$, i.e., at depolarized membrane potentials (Fig. 7). Furthermore, with respect to the gating pattern it is indicated from the current recordings in Fig. 7, which show brief channel closures (<50 msec) during long open-state periods (0.5–5 sec), that the dwell times of the closed state exhibit more than a single exponential distribution.

Unresolvable Chloride Channels

Some patches exhibited noisy currents with no resolvable channel events. As an example, Fig. 8*A* shows digitized current records obtained at nine different pipette potentials in an excised inside-out patch from the neck of

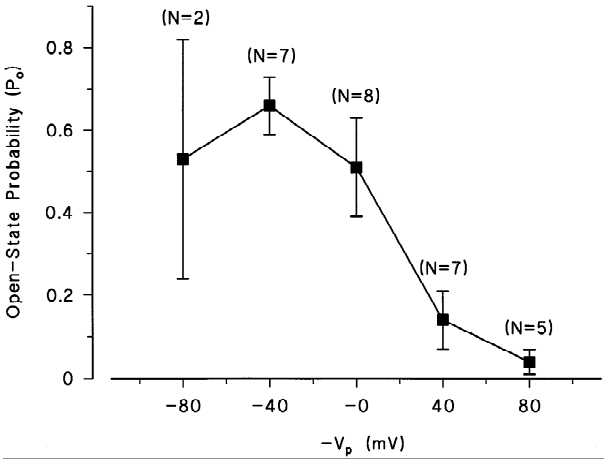

Fig. 6. Variation of the open-state probability for the intermediate Cl^- channel with membrane potential ($-V_p$) obtained from current traces as the ones shown in Fig. 5. Each point is indicating the mean P_o obtained with in a range of 40 mV, with the vertical lines indicating the SEM, and *N* the number of observations.

an MR cell. Assuming a homogenous population of *N* channels with open probability, P_o, and single channel current, *i*, the current, $\bar{i}$, flowing through open ion channels is given by,

$$\bar{i} = N \cdot P_o \cdot i = i_{patch} - g_{leak} \cdot (-V_p + V_{ij}) \qquad (12)$$

where i_{patch} is the current recorded from the patch, g_{leak} is the conductance of gigaseal, and V_{lj} is the liquid junction potential. The g_{leak} was estimated from current segments of minimal fluctuations (arrows in Fig. 9*A*), which we assume represent the residual current when all channels are closed. The current-voltage relationship of the seal and the calculated (Eq. 12) $\bar{i}/-V_p$ relationship of open channels in the patched membrane are depicted in Fig. 8*B*. It can be seen that the reversal potential of channel currents is, $V_{rev} \approx E_{Cl} - V_{ij}$, and that the current fluctuations (Figs. 8*A* and 9*A*) were practically abolished when V_p was clamped at $E_{Cl} - V_{lj}$. These observations indicate that the patch contains Cl^- channels, and that the noise is associated with current flow in these channels which open and close in a random fashion. Accordingly, we expect that the relationship between the variance of current fluctuations (σ^2) and the driving force imposed on the chloride ion flow through the channel would be parabolic and given by (conf. Eq. 10),

$$\sigma^2 = [N \cdot P_o \cdot (1 - P_o) \cdot \gamma^2] \cdot (-V_p + V_{ij} - E_{Cl})^2 \qquad (13)$$

This was tested by varying the pipette potential in steps of 20 mV in the range, −80 mV $\leqslant V_p \leqslant$ +80 mV, and recording currents at each V_p of sufficient duration for estimating the variance of their fluctuations (Fig. 9*A;* Materials and Methods, Eq. 9). As can be seen from three examples given in Fig. 9*B*, the fluctuations appear stationary throughout the 20-sec observation periods. The parabolic relationship between estimated current variance and pipette potential (Fig. 9*C*) supports the hypothesis that this patch contained unresolvable Cl^- channels. Figure 9*D* shows examples of calculated power density spectra. With the driving force on the chloride ion flow clamped at ~0 mV the spectrum is almost flat with a power which is no more than about 10× the background noise contributed from the patch-clamp amplifier (the 'Johnson noise' of the head-stage's 10 Gohm feedback resistor). The much larger Cl^- currents measured at, $-V_p = 80$ mV, exhibited a power spectrum which can be fitted by the sum of two Lorentzian functions (Eq. 10) as shown in Fig. 9*D*. The Lorentzian parameters together with the derived kinetic constants are listed in Table 1. The estimated relaxation time constants (Eqs. 11*A* and *B*) indicate fairly long durations of elementary currents. Thus, this analysis leads to the conclusion that the lack of kinetic steps in the recordings (Figs. 8*A* and 9*A*) is not due to a bandwidth limited frequency responses but, rather, to elementary currents which are too small for being resolved. The Gaussian distribution of digitized currents sampled during periods with 'all-channels-closed' in Fig. 2, and the calculated variance of the background noise records, $\sigma^2 = 0.007$ pA^2 (Fig. 9*A*), result in a similar estimate of the standard deviation (SD) of leak current distributions, i.e., SD ≈ 85 fA ($-V_p < 0$). Thus, we should be able to resolve step-current transitions of, $\Delta i \geqslant 170$ fA (2 · SD, signal filtered at, $f_c =$ 500 Hz). Accordingly, for the largest driving force imposed on the chloride ions, −100 mV ($V_p = -80$ mV), the single channel conductance would have been, $\gamma_{Cl} <$ 1.7 pS.

Discussion

This is the first study of single anion channels in the basolateral membrane of the mitochondria-rich cell, which constitute a minority cell type in vertebrate osmoregulatory epithelia. We have found that the two major populations comprise anion channels with a limiting conductance ($\gamma_{125/125}$) of ~10 pS and ~30 pS, respectively. They are both of the Ohmic type, i.e., within the physiological range of membrane potentials they do not show nonlinearities in excess of GHK-rectification. Occasionally, two other types of anion channels were observed. A large Ohmic 150-pS channel, and a small unresolvable channel with a conductance, $\gamma_{Cl} < 1.7$ pS. In the section following immediately below, we first discuss the finding that some of the channels identified in the present study possess poor anion selectivity, and we will compare the above channels with channels observed in other epithelial membranes, including the apical membrane of MR cells, with which they seem to share some biophysical features. Thus, we next discuss whether, in our

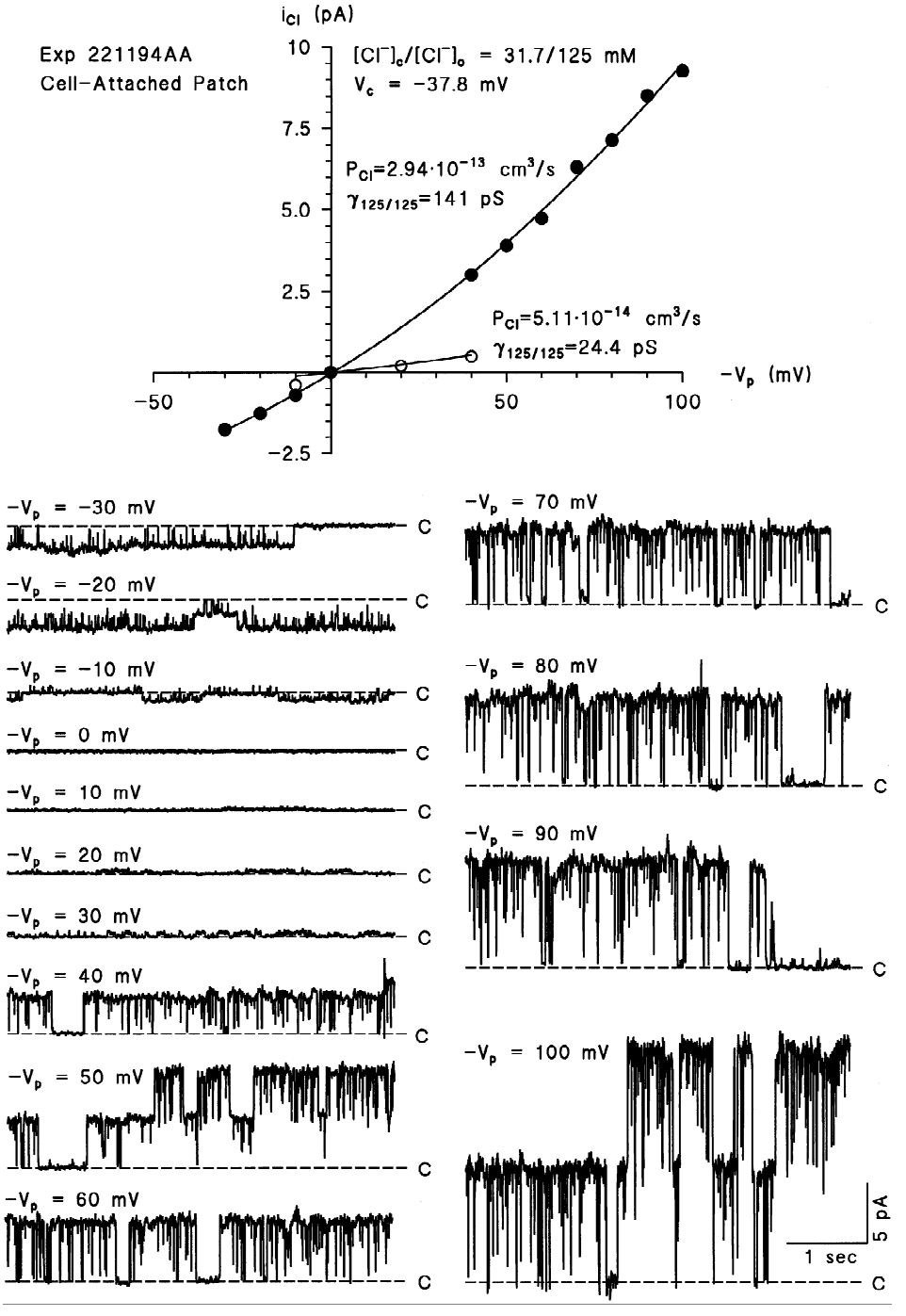

Fig. 7. Single-channel data from an cell-attached patch of the basolateral membrane containing two large Cl^- channels and an intermediate Cl^- channel. The best GHK fits of the $i_{Cl}/-V_p$ relations was obtained with V_c = −37.8 mV, $[Cl^-]_c$ = 31.7 mM, and a P_{Cl} of 29.4 × 10^{-14} cm^3/sec which translated into an $\gamma_{125/125}$ of 141 pS. The intermediate Cl^- channel was fitted with a permeability coefficient, P_{Cl} = 5.11 × 10^{-14} cm^3/sec corresponding to $\gamma_{125/125}$ = 28.4 pS.

preparation of isolated cells, channels of the apical and basolateral membrane domains have been mixed. Another important issue regards the confrontation of the apparent Cl^- conductance of the basolateral membrane inferred from the present study with that required in case previously measured macroscopic Cl^- currents in the intact epithelium are confined to mitochondria-rich cells. Finally, we will consider the possibility that electrically

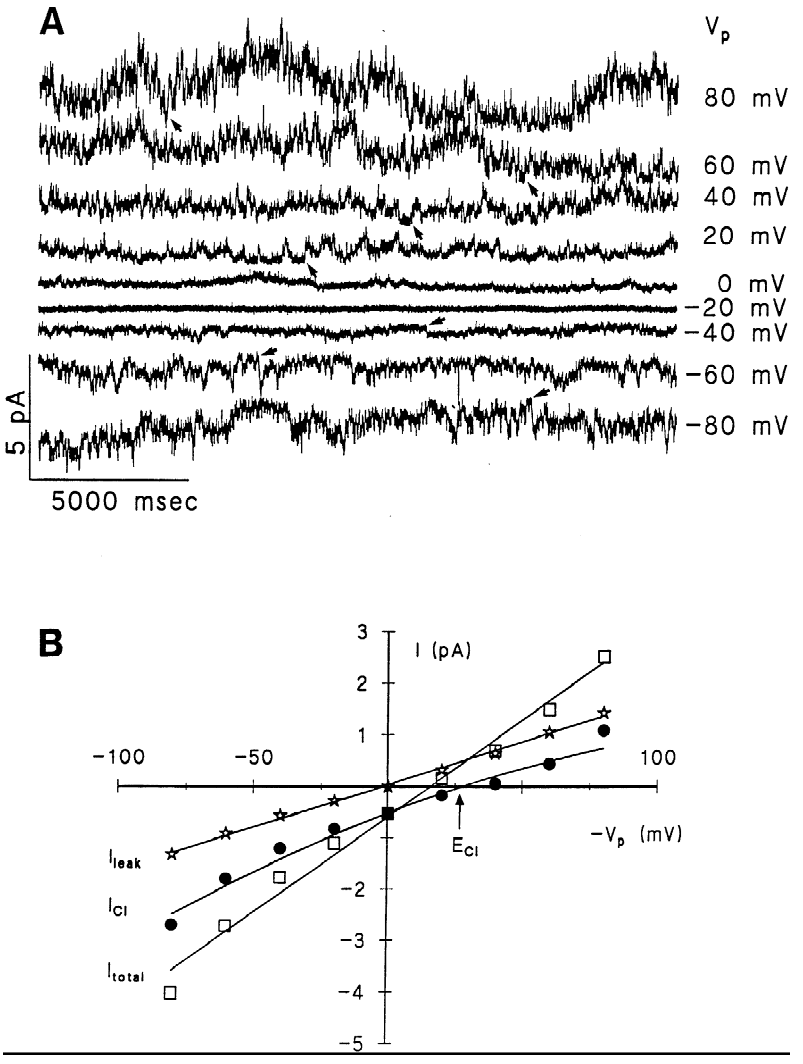

Fig. 8. (*A*) Original current recordings at $-V_p$ varying from −80 to 80 mV. Arrows indicate currents assumed to represent the all-channels-closed state used for construction of the $i_{leak}/-V_p$ relationship. (*B*) Relationships of $i_{leak}/-V_p$, $i_{patch}/-V_p$, and $\bar{i}/-V_p$, respectively. The $\bar{i}$ values were calculated from Eq. 3 and were fitted by the GHK equation (Eq. 1).

active Cl^- channels are not randomly distributed on the basolateral membrane, but organized in clusters.

Selectivity and Occurrence of Basolateral Anion Channels

In the presence of asymmetric, $[Cl^-]_p/[Cl^-]_o$ = 42/125 mM solutions (E_{Cl} = 27 mV), currents flowing through the 10 pS channel reversed at, $-V_p$ = 11.4 ± 1.9 mV (N = 5), which corresponds to about 19 mV, when corrected for a liquid junction potential of 7.5 mV. Interestingly, the 30 pS channel had a reversal potential of similar magnitude. This deviation of 8–9 mV from the reversal potential of a perfectly Cl^--selective channel indicates that the channels, besides Cl^-, are conductive to another ion as well, most likely gluconate which is the only other anion at a significant concentration. In that case the selectivity-ratio for the gluconate:Cl ion pair may be estimated from the equation:

$$\frac{P_{glu}}{P_{Cl}} = -\frac{[Cl^-]_p - [Cl^-]_b \cdot \exp(-\zeta \cdot V_{rev})}{[\text{gluconate}^-]_p} \quad (14)$$

where subscripts '*p*' and '*b*' refer to 'pipette' and 'bath', respectively. With $[\text{gluconate}]_p$ = 83.1 mM, $[Cl^-]_p$ = 41.6 mM, $[Cl^-]_b$ = 124.7 mM, and $V_{rev} \approx 19$ mV, we obtain a selectivity ratio of, $P_{glu}:P_{Cl} \approx 0.21$. This number is somewhat larger than the $P_{glu}:P_{Cl}$ ratio of the poorly anion selective 64 and 362 pS channels in the basolateral membrane of principal cells of the rabbit urinary bladder epithelium which have identical selectivity sequences, $Cl^- \approx Br^- \approx I^- \approx SCN^- \approx NO_3^- > F^-$ > acetate > gluconate, but with $P_{glu}:P_{Cl}$ = 0.07 and $P_{acetate}:P_{Cl}$ = 0.3 (Hanrahan et al., 1985). Anion channels of a similar poor anion

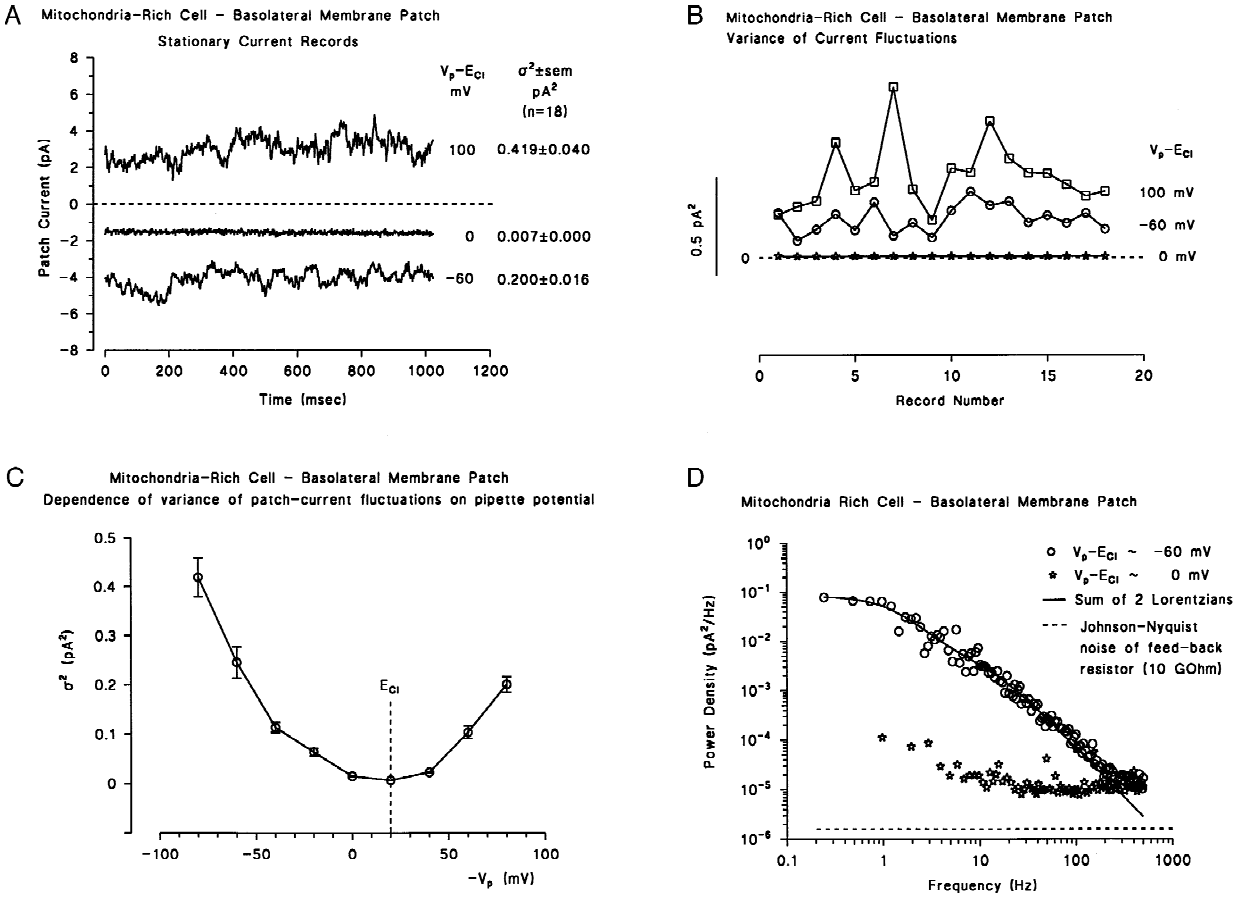

Fig. 9. (*A*) Current records at three different pipette potentials showing fluctuations with no resolvable single-channel events. (*B*) Variance of the stationary current fluctuations throughout the $-V_p$ range ±80 mV. Note that the variance is minimal close to the equilibrium potential for Cl^-. (*C*) Variance of the 18 consecutive records at three different $-V_p$ values (*see* Materials and Methods). (*D*) Cl^- current noise spectra obtained at a $-V_p$ of 0 and 80 mV, respectively, together with the background Johnson-noise of the patch-clamp amplifier. The sum of two Lorentzian functions indicated by the full line was calculated with the following parameters (Eq. 10), $f_{c1} = 1.24$ Hz, $S_{01} = 0.08$ pA^2/Hz and $f_{c2} = 13.1$ Hz, $S_{01} = 0.0034$ pA^2/Hz, respectively.

Table 1. Lorentzian parameters obtained from current fluctuation analysis of unresolvable Cl^- channels ($-V_p = 80$ mV, spectrum of Fig. 7D).

Lorentzian component	f_c Hz	S_o pA^2/Hz	σ^2 pA^2	τ msec	τ_{open} ($P_o = 0.5$) msec
I	1.24	0.080	0.156	128	256
II	13.1	0.0034	0.070	12	24

Variance (Eq. 10) and estimated mean opentimes (assuming $P_o = 0.5$; Eqs. 11A and B) are listed for the two Lorentzian components.

selectivity were inferred from a study of cell volume regulation in frog skin principal cells (Ussing, 1988). This last mentioned study of cells *in situ* indicated a relatively large permeability for Cl^-, Br^-, I^-, SCN^-, and NO_3^- of the basolateral anion channels activated during the regulatory volume decrease.

The most thoroughly studied 7–10 pS, Ohmic epithelial Cl^- channel is the cAMP-activated cystic fibrosis transmembrane conductance regulator (CFTR; Riordan et al., 1989). It has been identified in several types of vertebrate epithelia including airways and intestine (Anderson et al., 1992), pancreatic duct (Gray et al., 1989), and cortical collecting duct principal cells (Ling & Kokko, 1992). CFTR exhibits a Cl^- conductance which is much larger than that of gluconate. It is interesting that a 10 pS Cl^- channel has also been reported from the basolateral membrane of the proximal tubule of *Ambystoma* kidney (Segal & Boulpaep, 1992). The gene encoding this last mentioned amphibian channel has not been cloned, and it is unknown whether or not it is related to the basolateral anion channel of the amphibian MR-cells identified in the present study.

Depolarization-activated, outwardly rectifying 30–40 pS Cl^- channels were first reported from airways

(Frizzell, Rechkemmer & Shoemaker, 1986; Welsh, 1986) and have subsequently been found in the apical membrane of, e.g., proximal tubule cells (Suzuki et al., 1991), submandibular gland ducts (Ishikawa & Cook, 1994), and in the basolateral cell membranes of the thick ascending limb of the Loop of Henle (Greger et al., 1990). The channels of intermediate conductance appear quite variable with respect to voltage-dependence. Some are being activated by depolarization, some by hyperpolarization, while the activity of still others is independent of membrane potential (for further discussion, *see* Anderson et al., 1992).

Maxi or 'giant' Cl^- channels have not been commonly reported from vertebrate epithelia, but have been identified in, e.g., the apical membrane of intercalated cells from the cortical collecting duct (305 pS, Light et al., 1990; Schwiebert et al., 1990) and trachea (100–120 pS, Duszyk et al., 1995); maxi Cl^- channels have also been identified in the apical membranes of confluent A6 kidney culture cells (360 pS, Nelson et al., 1984), and MDCK cells (456 pS, Kolb, Brown & Murer, 1985). Their presence in mitochondria-rich cells was first indicated in a study of the noise generated by depolarization activated whole cell Cl^- currents (Larsen & Harvey, 1994). In our subsequent single channel study, similar 'giant' Cl^- channels were active in a minority of apical membrane patches (Sørensen & Larsen, 1996).

Unresolvable and slowly gated Cl^- channels were first described in a study of isolated rat lacrimal gland cells. They were activated via increase in the cytosolic $[Ca^{2+}]$ accomplished either by cholinergic receptor occupation or by A23187-exposure (Marty, Tan & Trautmann, 1984). Chloride currents generated by unresolvable channels have also been recorded from the apical membrane of HT_{29} colon carcinoma cells (Kubitz et al., 1992; Kunzelmann et al., 1992; Disser, Hazama & Frömter, 1993) and bronchial cells (Kunzelmann et al., 1994), where they were activated by intracellular cAMP, or by PKA-mediated phosphorylation of excised inside-out membrane patches. In the apical (Sørensen & Larsen, 1996) and basolateral membrane (present study) of mitochondria-rich cells, unresolvable Cl^- channels occurred with a low frequency, but without prior stimulation.

Functional Polarity of Isolated Mitochondria-Rich Cells

The basolateral Cl^- channels identified in the present study share several features with those of the apical membrane characterized in a recent study of our MR-cell preparation (Sørensen & Larsen, 1996). In both membrane domains is the Cl^- channel most commonly encountered an Ohmic, voltage-independent 10 pS channel. Furthermore, the apical membrane contained a rather inhomogeneous group of voltage-dependent 10–30 pS Cl^- channels and a large, highly variable 150–550 pS channel exhibiting multiple substates. Finally, the apical membrane also contains unresolvable Cl^- channels. The above findings raise the question whether, in isolated cells, channel proteins of the apical and basolateral membrane domains interchange by lateral diffusion. Epithelial cells have been found to lose their polarity upon removal of external Ca^{2+} (Contreras et al., 1992; Torres et al., 1996), and although the exposure time to the Ca^{2+}-free solution in our study was brief (*see* Materials and Methods), we have to consider whether our isolation procedure causes loss of functional polarity.

Several observations make it unlikely, but do not definitively exclude that membrane channels of the apical and basolateral membrane domains have been mixed. (*i*) The cytoskeleton, supposed to provide anchoring for integral membrane proteins, appears unmodified as indicated by the maintenance of the characteristic flasklike shape of isolated MR-cells (*see* Fig. 1 in Larsen and Harvey (1994), and Fig. 1*B* of the present study). (*ii*) The intermediate anion channel in the basolateral membrane is Ohmic and activated by hyperpolarization (Fig. 6). In the apical membrane, the channel of similar conductance is slightly outwardly rectifying, and activated by depolarization. (*iii*) The 10 pS basolateral anion channel exhibits a relatively high gluconate permeability (conf. above). In contrast, the 7–10 pS apical channel does not reveal any measurable gluconate permeability. (*iv*) The basolateral 150 pS Cl^- channel identified in the present study was characterized by conductance transitions of a uniform amplitude with no indications of conductive substates (Fig. 7). The large 150–500 pS Cl^- channel of the apical membrane exhibit multiple conductive substates.

Thus, it should be clear that the channels of the basolateral and the apical membrane, respectively, are sufficiently different for concluding that unless the channels become modified following diffusion from one membrane domain to the other, there is no obvious indication of loss of functional polarity.

Relationship to Transepithelial Chloride Fluxes

The various basolateral channels of the MR cell may serve different cellular functions as, for example, volume regulation, transport of Cl^- associated with apical cAMP conductance activation, transport of HCO_3^- or small organic anions, transport of Cl^- which have entered the cell either via active uptake from the outside solution, or as result of voltage activation of the passive Cl^- uptake.

If a single population of basolateral channels is carrying the membrane current, I_{Cl} is related to the single-channel conductance by,

$$I_{Cl} = N \cdot P_o \cdot \gamma_{Cl} \cdot (V_m - E_{Cl}) \quad (15)$$

where N is the number of basolateral Cl^- channels in a

Table 2. Summary of data for Cl^- channels identified in basolateral MR cell membranes of toad skin epithelium

Channel type	Frequency, λ_p %	Single channel P_{Cl} 10^{-14} cm^3/sec	$\gamma_{125/125}$ pS	# of channels per patch, $\overline{N}$
Small	43	2.22 ± 0.12	10.5 ± 0.29	2.11 ± 0.29
Intermediate	39	5.74 ± 0.73	30.6 ± 1.4	1.44 ± 0.32
Large	9	32.4 ± 1.9	154 ± 9	2.00 ± 0.71
Unresolvable	9		<1.7	Multiple

Values are presented as mean ± SEM.

cell, γ_{Cl} is the integral single-channel conductance (Eq. 3), and P_o is the open probability. The number of active Cl^- channels per cell, N in Eq. 15, is given by the equation,

$$N = \lambda_p \cdot \lambda \cdot \left(\frac{A_{MRC}}{A_{patch}}\right) \cdot \overline{N}_{patch} \quad (16)$$

where λ_p is the frequency of active patches (0.322, *see* Results), λ the frequency of active patches expressing the channel considered (Table 1), A_{MRC} the area of the basolateral membrane of an MR cell (which can be estimated from Fig. 1*B* and *C*), A_{patch}, the area of the patch membrane (estimated from Fig. 1*A*), and $\overline{N}_{patch}$ the mean number of the channel considered per active patch (Table 2). From such an estimate we can calculate (Eq. 15) that the three types of resolvable channels would account for macroscopic whole-cell currents (I_{Cl}) of no more than 0.046, 0.089, and 0.144 nA, respectively, or about one order of magnitude lower than the observed fully activated whole-cell Cl^- currents. Such a discrepancy between micro- and macroscopic MR cell Cl^- currents was also reported in a recent study of apical Cl^- channels of MR cells (Sørensen & Larsen, 1997), and it indicates that Cl^- channels may be inactivated or lost, e.g., by degradation or internalization during the cell isolation procedure.

Evidence for Clustering of Basolateral Anion Selective Channels

As the active patches constituted only 32% of all patches studied, we would expect that the majority of active patches contained no more than a single channel. To our surprise, however, the present study has shown that many of the active patches contained more than a single copy of a given Cl^- channel. For example, one patch contained no less than four active 30 pS channels. Given the frequency of active patches and the frequency of the 30 pS channel in active patches, the probability of finding four 30 pS channels in the same patch, assuming that the channels were evenly distributed in the membrane, would be 0.00013. This indicates that the active channels are not evenly distributed in the basolateral membrane but, rather, they occur in clusters. Clustering of membrane channels has recently been proposed (Mazzanti et al., 1991; Stutts et al., 1995; Al-Awqati, 1995; Larsen et al., 1996). However, the fact that both the 10 pS and the 30 pS channels were detected in the MR cell soma and neck indicates no large-scale spatial inhomogeneity, i.e., the channels appear to be confined neither to neck nor to soma of the mitochondria-rich cell.

The authors wish to thank Ms. Birthe Petersen, Ms. Anni Olsen and Ms. Hanne Schaltz for expert assistance in the laboratory preparing isolated MR cells. This study was supported by the Danish Natural Science Research Council, and the Alfred Benzon, Carlsberg, and Novo Nordisk Foundations.

References

Al-Awqati, Q. 1995. Regulation of ion channels by ABC transporters that secrete ATP. *Science* **269:**805–806

Anderson, M.P., Sheppard, D.N., Berger, H.A., Welsh, M.J. 1992. Chloride channels in the apical membrane of normal and cystic fibrosis airway and intestinal epithelia. *Am. J. Physiol.* **263:**L1–L14

Barry, P.H., Lynch, J.W. 1991. Liquid junction potentials and small cell effects in patch-clamp analysis. *J. Membrane. Biol.* **121:**101–117

Bijman, J., Frömter, E. 1986. Direct demonstration of high transepithelial chloride-conductance in normal human sweat duct which is absent in cystic fibrosis. *Pfluegers Arch.* **407:**S123–S127

Contreras, R.G., Gonsález-Mariscal, L., Balda, M.S., García-Villegas, M.R., Cereijido, M. 1992. The role of calcium in the making of a transporting epithelium. *NIPS* **7:**105–108

Disser, J., Hazama, A., Frömter, E. 1993. Chloride channel studies on HT_{29} cells with Minimal levels of cAMP-mediated stimulation. *Pfluegers Arch.* **422:**R65 (Abstr.)

Duszyk, M., Liu, D., Kaminowska, B., French, A.S., Paul Man, S.F. 1995. Characterization and regulation of a chloride channel from bovine tracheal epithelium. *J. Physiol.* **489:**81–93

Finkelstein, A., Mauro, A. 1963. Equivalent circuits as related to ionic systems. *Biophys. J.* **3:**215–237

Foskett, K.J., Ussing, H.H. 1986. Localization of chloride conductance to mitochondria-rich cells in frog skin epithelium. *J. Membrane Biol.* **91:**251–258

Foskett, K.J., Bern, H.A., Machen, T.E., Conner, M. 1983. Chloride cells and the hormonal control of teleost fish osmoregulation. *J. Exp. Biol.* **106:**255–281

Frizzell, R.A., Rechkemmer, G., Shoemaker, R.L. 1986. Altered regulation of airway epithelial cell chloride channels in cystic fibrosis. *Science* **233:**558–560

Goldman, D.E. 1943. Potential, impedance, and rectification in membranes. *J. Gen. Physiol.* **27:**37–60

Gray, M.A., Harris, A., Coleman, L., Greenwell, J.R., Argent, B.E. 1989. Two types of chloride channels on duct cells cultured from human fetal pancreas. *Am. J. Physiol.* **257:**C240–C251

Greger, R., Bleich, M., Schlatter, E. 1990. Ion channels in the thick ascending limb of Henle's loop. *Renal Physiol. and Biochem.* **13:**37–50

Hanrahan, J.W., Alles, W.P., Lewis, S.A. 1985. Single anion-selective channels in the basolateral membrane of a mammalian tight epithelium. Proc. Natl. Acad. Sci. USA **82:**7791–7795

Harck, A.F., Larsen, E.H. 1986. Concentration dependence of halide fluxes and selectivity of the anion pathway in toad skin. *Acta Physiol. Scand.* **128:**289–304

Hille, B. 1984. Ionic channels of excitable membranes. pp. 1–426. Sinauer Associates, Sunderland, MA

Hodgkin, A.L., Katz, B. 1949. The effect of sodium ions on the electrical activity of the giant axon of the squid. *J. Physiol.* **102:**37–77

Ishikawa, T., Cook D.I. 1994. Characterization of an outward rectifying chloride channel in a human submandibular gland duct cell line (HSG). *Pfluegers Arch.* **427:**203–209

Jensen, L.J., Sørensen, J.N., Larsen, E.H., Willumsen, N.J. 1997. Proton pump activity of mitochondria-rich cells: the interpretation of external proton-concentration gradients. *J. Gen. Physiol.* **109:**73–91

Katz, U., Gabbay, S. 1988. Mitochondria-rich cells and carbonic anhydrase content of toad skin epithelium. *Cell Tissue Res.* **251:**425–431

Katz, U., Scheffey, C. 1986. The voltage-dependent chloride conductance of toad skin is localized to mitochondria-rich cells. *Biochim. Biophys. Acta* **861:**480–482

Kolb, H.A., Brown, C.D.A., Murer, H. 1985. Identification of a voltage-dependent anion channel in the apical membrane of a Cl^- secretory epithelium (MDCK). *Pfluegers Arch.* **403:**262–265

Krogh, A. 1937. Osmotic regulation in the frog (*R. esculenta*) by active absorption of chloride ions. *Skand. Arch. Physiol.* **76:**60–74

Kubitz, R., Warth, R., Allert, M., Kunzelmann, K., Greger, R. 1992. Small conductance chloride channels induced by cAMP, Ca^{2+}, and hypertonicity in HT_{29} cells: ion selectivity, additivity, and stilbene sensitivity. *Pfluegers Arch.* **421:**447–454

Kunzelmann, K., Grolik, M., Kubitz, R., Greger, R. 1992. cAMP-dependent activation of small-conductance Cl^- channels in HT_{29} colonic carcinoma cells. *Pfluegers Arch.* **421:**230–237

Kunzelmann, K., Kolowski, T., Hug, T., Gruenert, D.C., Greger, R. 1994. cAMP-dependent activation of ion conductances in bronchial epithelial cells. *Pfluegers Arch.* **428:**590–596

Larsen, E.H., Christoffersen, B.C., Jensen, L.J., Sørensen, J.B., Willumsen, N.J. 1995. Role of mitochondria-rich cells for epithelial chloride uptake. *J. Physiol.* **81:**525–534

Larsen, E.H., Harvey, B.J. 1994. Chloride currents of single mitochondria-rich cells of toad skin epithelium. *J. Physiol.* **478:**7–15

Larsen, E.H., Kristensen, P. 1978. Properties of a conductive chloride pathway in the skin of the toad (*Bufo bufo*). *Acta Physiol. Scand.* **102:**1–21

Larsen, E.H., Price, E.M., Gabriel, S.E., Stutts, M.J., Boucher, R.C. 1996. Clusters of Cl^- channels in CFTR-expressing Sf9 cells switch spontaneously between slow and fast gating modes. *Pfluegers Arch.* **432:**528–537

Larsen, E.H., Ussing, H.H., Spring, K.R. 1987. Ion transport by mitochondria-rich cells in toad skin. *J. Membrane Biol.* **99:**25–40

Larsen, E.H., Willumsen, N.J., Christoffersen, B.C. 1992. Role of proton pump of mitochondria-rich cells for active transport of chloride ions in toad skin epithelium. *J. Physiol.* **450:**203–216

Light, D.B., Schwiebert, E.M., Fejes-Toth, G., Naray-Fejes-Toth, A., Karlson, K.H., McCann, F.V., Stanton, B.A. 1990. Chloride channels in the apical membrane of cortical collecting duct cells. *Am. J. Physiol.* **258:**F273–F280

Ling, B.N., Kokko, K.E. 1992. PGE_2 activates apical chloride channels in rabbit cortical collecting tubule (RCCT) principal cells via a cAMP-dependent pathway. *J. Am. Soc. Nephrol.* **3:**813 (*Abstr.*).

Marty, A., Tan, Y.P., Trautmann, A. 1984. Three types of calcium-dependent channel in rat lacrimal glands. *J. Physiol.* **357:**293–325

Mazzanti, M., DeFelice, L.J., Liu, Y.-M. 1991. Gating of L-type Ca^{2+} channels in embryonic chick ventricle cells: dependence on voltage, current, and channel density. *J. Physiol.* **443:**307–334

Neher, E. 1992. Correction for liquid junction potentials in patch clamp experiments. *Methods in Enzymol.* **207:**123–131

Nelson, D., Tang, J.M., Palmer, L.G. 1984. Single-channel recordings of apical membrane chloride conductance in A6 epithelial cells. *J. Membrane Biol.* **80:**81–89

Rick, R. 1994. Short-term bromide uptake in skins of *Rana pipiens*. *J. Membrane Biol.* **138:**171–179

Riordan, J.R., Rommens, J.M., Kerem, B.-S., Alon, N., Rozmahel, R., Grzelczak, Z., Zielenski, J., Lok, S., Plavsic, N., Chou, J.-L., Drumm, M.L., Iannuzzi, M.C., Collins, F.S., Tsui, L.-C. 1989. Identification of the cystic fibrosis gene: cloning and characterization of complementary DNA. *Science* **245:**1066–1073

Schwiebert, E.M., Light, D.B., Fejes-Toth, G., Naray-Fejes-Toth, A., Stanton, B.A. 1990. A GTP-binding protein activates chloride channels in a renal epithelium. *J. Biol. Chem.* **265:**7725–7728

Schwiebert, E.M., Mills, J.W., Stanton, B.A. 1994. The actin-based cytoskeleton regulates a chloride channel and cell volume in renal cortical collecting duct cell line. *J. Biol. Chem.* **269:**7081–7089

Segal, A.S., Boulpaep, E.L. 1992. cAMP-activated chloride channel on the basolateral membrane of renal proximal tubule. *J. Am. Soc. Nephrol.* **3:**819 (*Abstr.*)

Stutts, M.J., Canessa, C.M., Olsen, J.C., Hamrick, M., Cohn, J.A., Rossier, B.C., Boucher, R.C. 1995. CFTR as a cAMP-dependent regulator of sodium channels. *Science* **269:**847–850

Suzuki, M., Morita, T., Hanaoka, K., Kawaguchi, Y., Sakai, O. 1991. A chloride channel activated by parathyroid hormone in rabbit renal proximal tubule cells. *J. Clin. Invest.* **88:**735–742

Sørensen, J.B., Larsen, E.H. 1996. Heterogeneity of chloride channels in the apical membrane of isolated mitochondria-rich cells from toad skin. *J. Gen. Physiol.* **108:**421–433

Torres, R.J., Altenberg, G.A., Copello, J.A., Zampighi, G., Reuss, L. 1996. Preservation of structural and functional polarity in isolated epithelial cells. *Am. J. Physiol.* **270:**C1864–C1874

Ussing, H.H. 1988. Anion transport pathways in frog skin epithelium. *In:* Molecular Mechanisms in Secretion. *Proc. Alfred Benzon Symposium* **25:**17–27. N.A. Thorn, M. Treiman, and O.H. Petersen, editors. Munksgaard, Copenhagen

Voûte, C.L., Meier, W. 1978. The mitochondria-rich cell of frog skin as hormone sensitive 'shunt path'. *J. Membrane Biol.* **40:**141–165

Welsh, M.J. 1986. An apical membrane chloride channel in human tracheal epithelium. *Science* **232:**1648–1650

Willumsen, N.J., Boucher, R.C. 1989. Shunt resistance and ion permeabilities in normal and cystic fibrosis airway epithelia. *Am. J. Physiol.* **256:**C1054–C1063

Willumsen, N.J., Larsen, E.H. 1986. Membrane potentials and intracellular Cl^- activity of toad skin epithelium in relation to activation and deactivation of the transepithelial Cl^- conductance. *J. Membrane Biol.* **94:**173–190

Willumsen, N.J., Larsen, E.H. 1995. Chloride channels in the basolateral membrane of mitochondria-rich cells of toad skin epithelium. *J. Physiol.* **489:**116P (*Abstr.*)

Willumsen, N.J., Larsen, E.H. 1996. Basolateral chloride channels of mitochondria-rich cells of toad skin epithelium. *FASEB J.* **10:**A75 (*Abstr.*)

Willumsen, N.J., Vestergaard, L.O., Larsen, E.H. 1992. Cyclic AMP- and β-agonist activated chloride conductance of a toad (*Bufo bufo*) skin epithelium. *J. Physiol.* **449:**641–653